Proceedings of the 25th International Conference on
Port and Ocean Engineering under Arctic Conditions
June 9-13, 2019, Delft, The Netherlands

Modelling the dynamics of ice in the Antarctic marginal ice zone

Rutger Marquart[1], Keith MacHutchon[1], Alfred Bogaers[2,3], Marcello Vichi[4], Sebastian Skatulla[1]

[1] University of Cape Town, Department of Civil Engineering, Cape Town, South Africa
[2] Ex Mente Technologies, Pretoria, South Africa
[3] School of Computer Science and Applied Mathematics, University of the Witwatersrand, Johannesburg, South Africa
[4] University of Cape Town, Department of Oceanography, Cape Town, South Africa

ABSTRACT

Hibler (1979) describes a sea ice model in which the internal ice stress and strain rate are related by means of a viscous-plastic sea ice rheology. A large sea ice area is modelled as an isotropic, continuous and homogeneous material (Hutchings, Jasak et al. 2004). This model considers pack ice as a single homogenized material with constant ice density, where ice thickness, ice coverage and ice velocity are the main variables. An existing large-scale numerical model, based on Hibler's model, has been implemented in the computational fluid dynamics software OpenFOAM by Bogaers, Rensburg et al. (2018). This paper reports on the modification to the large-scale OpenFOAM model to develop a small-scale sea ice model, considering a material composition consisting of separately pancake ice and frazil ice with distinct properties. The thermodynamics of sea ice is neglected, since only small time periods are modelled. Pancake-frazil and pancake-pancake ice interactions are analysed. Wind and ocean current are applied (Mehlmann and Richter 2017). Average stress, strain rate and viscosities are obtained.

KEY WORDS: Hibler’s model; Sea ice rheology; Large and small-scale; Material parameters

INTRODUCTION

Sea ice plays a significant role in the global climate and covers approximately 10% of the earth's surface (Wilchinsky and Feltham 2006). Understanding sea ice dynamics and thermodynamics results in better sea ice predictions and therefore a better comprehension of the Antarctic marginal ice zone (MIZ) (Herman 2016). Large-scale sea ice models have been developed to operate successfully at length scales of 10 to 100 kilometers-domain size. Finer-scale models of sea ice dynamics are scarce (Dansereau, Weiss et al. 2016), in particular with respect to the characteristic pancake ice found in the Antarctic MIZ.

Sea ice has a major impact on the global climate and life of marine organisms in and below the ice (Massom and Stammerjohn 2010). The ice acts as a layer between the ocean and atmosphere and dominates the heat, gas and momentum exchange (Thorndike, Rothrock et al. 1975). Large ocean heat losses occur due to leads, which are cracks in the ice cover. Relatively warm water below the thin ice layer is exposed to the cold atmosphere (Kantha 1995). The extent to which ice has an impact on heat loss, depends on the distribution of the ice coverage, thickness, dynamics, ice type and snow coverage (Massom and Stammerjohn 2010). This paper focusses on the dynamics of sea ice, considering specifically the solid and fluid mechanics of sea ice.

Several sea ice models have been developed in the past, the majority of which are large-scale models. One of these models is developed by Hibler, which is largely recognized as the standard sea ice dynamics model. In this model, the viscous-plastic sea ice rheology relates the internal ice stress and strain rate. A large fractured sea ice area is modelled as an isotropic, continuous and homogeneous material (Hutchings, Jasak et al. 2004). In the case of consolidated ice with constant ice density, the main variables are ice thickness, ice coverage and ice velocity. Most large-scale models represent an ice-covered area at length scales of 10 to 100 kilometers (Bogaers, Rensburg et al. 2018). This is the scale at which the material laws have been developed and verified. The response at these levels, given the chosen models, tend to be representative. These models use a smeared model approach, in which several different types of ice are modelled as one homogeneous material, representing averaged quantities. Sea ice models on a smaller scale are scarce (Dansereau, Weiss et al. 2016), in particular with respect to the characteristic pancake ice found in the Antarctic MIZ. For this reason, we have developed a small-scale model, where the pancake ice and frazil ice are treated with distinct material properties.

Sea ice modelling has been helpful in gaining a better understanding of the polar regions, however, most of these models are based on the Arctic. Research in the Arctic is more accessible, since weather conditions are less severe, and it is less remotely located. Hence, understanding sea ice behaviour in the Antarctic MIZ still requires some attention.

LARGE-SCALE MODEL

The viscous-plastic sea ice model is based on the model previously developed by Coon (1980). He replaced the elastic behaviour in the constitutive equation by the viscous behaviour to eliminate the need to update the geometry when computing the strain (Feltham 2008). Only thick and thin ice are considered, which includes open water, with an ice concentration, A, quantified by an area fraction between 0 and 1 where the latter stands for 100% ice coverage, often referred to as consolidated ice.

Using an inelastic material law with an elliptical yield curve, shown in Figure 1, Hibler proved that the relationship between average stress and strain rate is linearly viscous, including a pressure term. According to Feltham (2008) this behaviour is caused by large variations between the strain rate and the mean strain rate.

The momentum equation is written as

$$m\left(\frac{\partial \boldsymbol{U}}{\partial t} + (\boldsymbol{U}\cdot\boldsymbol{\nabla})\boldsymbol{U}\right) = \boldsymbol{\tau}_a + \boldsymbol{\tau}_w - mf\boldsymbol{k}\times\boldsymbol{U} - mg\boldsymbol{\nabla}H + \boldsymbol{\nabla}\cdot\boldsymbol{\sigma}, \quad (1)$$

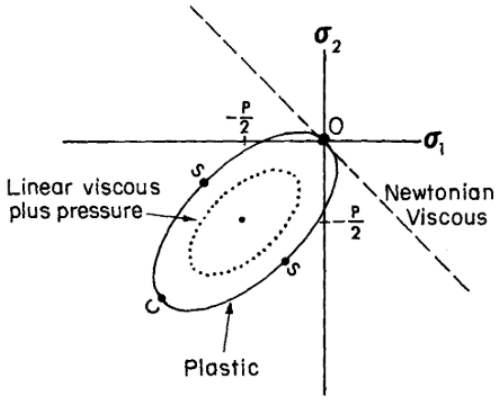

Figure 1. Viscous-plastic yield curve by Hibler (1979).

which links internal and external forces. The wind, current, Coriolis and pressure gradient represent the external forces. The internal reaction forces represented by the Cauchy stress tensor, $\boldsymbol{\sigma}$, have a highly non-linear dependency on a variety of sub-scale interactions (Bogaers, Rensburg et al. 2018). $\boldsymbol{U}$ represents ice velocity and m the mass of ice. Wind and ocean current stress vectors applied to the ice are represented by $\boldsymbol{\tau}_a$ and $\boldsymbol{\tau}_w$, respectively. f is the Coriolis parameter and $\boldsymbol{k}$ represents a unit normal vector to the surface of the ice. g and H represent gravitational acceleration and sea surface dynamic height, respectively.

Both wind and current stress are written as

$$\boldsymbol{\tau}_a = \rho_a C_a |\boldsymbol{U}_a| (\boldsymbol{U}_a \cos\theta_a + \boldsymbol{k} \times \boldsymbol{U}_a \sin\theta_a), \tag{2}$$

$$\boldsymbol{\tau}_w = \rho_w C_w |\boldsymbol{U}_w - \boldsymbol{U}| ((\boldsymbol{U}_w - \boldsymbol{U}) \cos\theta_w + (\boldsymbol{U}_w - \boldsymbol{U}) \boldsymbol{k} \times \boldsymbol{U}_w \sin\theta_w), \tag{3}$$

where variables $\boldsymbol{U}_a$ and $\boldsymbol{U}_w$ respectively represent wind and ocean current velocities. The material parameters for air and water are their densities ρ_a and ρ_w, respectively, drag coefficients C_a and C_w, and turning angles θ_a and θ_w.

The ice mass is determined by $m = \rho_i h$, where ρ_i and h represent ice density and ice thickness, respectively. In the case of open water, ice thickness equals zero, which results in an ill-posed and thus unsolvable momentum equation. Hence, a lower limit has been introduced on the sea ice thickness of $h = 0.5$m. However, this is rather unrealistic, and therefore Bogaers, Rensburg et al. (2018) considered zero ice thickness, which in this case requires solving for a sea ice velocity which satisfies the condition $\boldsymbol{\tau}_a + \boldsymbol{\tau}_w = 0$, which can be achieved by solving for a water shear stress of

$$\begin{aligned} \boldsymbol{\tau}_w = &-\rho_w C_w |\boldsymbol{U}_w - \boldsymbol{U}| \cos\theta_w \boldsymbol{U} \\ &+ \rho_w C_w |\boldsymbol{U}_w - \boldsymbol{U}| \big((\boldsymbol{U}_w) \cos\theta_w + (\boldsymbol{U}_w - \boldsymbol{U}) \widehat{\boldsymbol{k}} \times \boldsymbol{U}_w \sin\theta_w \big). \end{aligned} \tag{4}$$

The viscous-plastic sea ice rheology describes the relationship between the sea ice stress tensor components, $\boldsymbol{\sigma}$, the sea ice strain rate tensor components, $\dot{\boldsymbol{\varepsilon}}$, and the internal ice strength P, governing its compressibility. The viscous-plastic constitutive law is given as

$$\boldsymbol{\sigma} = 2\eta \dot{\boldsymbol{\varepsilon}} + \boldsymbol{I} \left[(\zeta - \eta) \mathrm{tr}(\dot{\boldsymbol{\varepsilon}}) - \frac{P}{2} \right], \tag{5}$$

which describes the homogeneous and isotropic behaviour of sea ice. The strain rate can be written in terms of the ice velocity $\boldsymbol{U}$,

$$\dot{\boldsymbol{\varepsilon}} = \frac{1}{2}(\boldsymbol{\nabla U} + (\boldsymbol{\nabla U})^T). \tag{6}$$

All terms in equation (5) linked to η represent the deviatoric part of the constitutive law. The ζ term represents the spherical part of the rate-dependent part of the constitutive law. The P term quantifies rate-independent compressibility behaviour. Both strain rate dependent viscosities, namely the deviatoric and spherical contributions, are coupled as given below:

$$\zeta = \frac{P}{2\Delta}, \qquad \eta = \frac{\zeta}{e^2}, \tag{7}$$

The strain rate dependent parameter Δ is defined as

$$\Delta = [(\dot{\varepsilon}_{11}^2 + \dot{\varepsilon}_{22}^2)(1 + e^{-2}) + 4e^{-2}\dot{\varepsilon}_{12}^2 + 2\dot{\varepsilon}_{11}\dot{\varepsilon}_{22}(1 - e^{-2})]^{\frac{1}{2}}, \tag{8}$$

where the ratio between the principle axis of the elliptical yield curve is represented by e and $\dot{\varepsilon}_{11}$, $\dot{\varepsilon}_{22}$ and $\dot{\varepsilon}_{12}$ denote the Cartesian components of the strain rate tensor.

As strain rates approach zero, the viscosity tends to infinity. To avoid this, a lower limit of the effective strain rate is imposed, $\Delta = 2 \cdot 10^{-9}$ s^{-1}. The ice does not behave completely as a rigid solid, but rather slowly creeps (Hunke and Dukowicz 1997).

The ice strength parameter P is given as

$$P = P^* h e^{-C(1-A)}, \tag{9}$$

which depends on ice thickness, h, ice coverage, A, and two empirical constants, P^* and C. The transport of ice thickness, h, and ice coverage, A, are defined by the advection transport equations as

$$\frac{\partial h}{\partial t} + \boldsymbol{\nabla} \cdot (h\boldsymbol{U}) = S_h, \qquad \frac{\partial A}{\partial t} + \boldsymbol{\nabla} \cdot (A\boldsymbol{U}) = S_A, \tag{10}$$

where S_h and S_A represent thermodynamic source terms, which are set to 0 for the purposes of the current study.

SMALL-SCALE MODEL

The primary aim of this work is to develop a small-scale model, which describes the dynamics of sea ice in the Antarctic MIZ. Hibler's existing large-scale model, implemented in OpenFOAM by Bogaers, Rensburg et al. (2018), is used as a basis, which is subsequently modified to obtain a more accurate and realistic model. To achieve this, the following objectives are set:

- Distinguish between two main material constituents, namely, pancake ice and frazil ice. All constituents are described by their own material law, each with different material characteristics. Correct implementation and analyses of the interaction of ice materials, e.g. pancake-pancake ice and pancake-frazil ice interactions is required.

- Implementation of wind, waves and ocean current.
- Find the transition from small-scale to large-scale sea ice models.

The choice of rheology is based on material characteristics of each constituent. Unlike the treatment in the viscous-plastic rheology of sea ice on the larger scale, single pancake ice modelling on the small-scale need to consider its dominantly solid-like behaviour, which results in small deformations. Therefore, pancake ice will be described using Hooke's law. Frazil ice behaves like a fluid, since it has no rigidity, and thus can be considered to be governed by viscous-plastic behaviour. Hence, the intended small-scale sea ice model will be described by an elastic-viscous-plastic rheology. Adding an elastic part to the re-written viscous-plastic rheology given in equation (5), results in the equation given below:

$$\frac{1}{E}\frac{\partial \boldsymbol{\sigma}}{\partial t} + \frac{1}{2\eta}\boldsymbol{\sigma} + \boldsymbol{I}\left[\frac{\eta - \zeta}{4\eta\zeta}\mathrm{tr}(\boldsymbol{\sigma}) + \frac{P}{4\zeta}\right] = \dot{\boldsymbol{\varepsilon}}. \tag{11}$$

By adding the elastic part to the equation, Hunke and Dukowicz (1997) used this EVP equation to solve the viscous-plastic rheology more accurate and efficient. Compared to the viscous-plastic model, this EVP rheology allows for solving the transient response more accurately using larger time steps. The transient response can be defined as any response to a change from steady-state conditions of the system. Hunke and Dukowicz (1997) solved this equation by writing it numerically as

$$\frac{1}{\Delta t}(\boldsymbol{\sigma}^{k+1} - \boldsymbol{\sigma}^{k}) + \frac{E}{2\eta}\boldsymbol{\sigma}^{k+1} + \boldsymbol{I}\left[E\frac{\eta - \zeta}{4\eta\zeta}\mathrm{tr}(\boldsymbol{\sigma}^{k+1}) + \frac{EP}{4\zeta}\right] = E\dot{\boldsymbol{\varepsilon}}^{k}, \tag{12}$$

where E represents the Young's modulus and k the iteration step of the discretised momentum equation for a time step size of Δt. Note, however, that Hunke and Dukowicz (1997) applied this approach to the large-scale domain considering one single homogenized material and the elastic term is added solely as a numerical stabilisation term.

As mentioned before, in contrast to Hunke and Dukowicz (1997), the proposed small-scale sea ice rheology considers a domain where pancake ice and frazil ice are geometrically distinguished from each other. Accordingly, the elastic part, representing pancake ice, is derived from Hooke's law in three dimensions, which can be written as

$$\boldsymbol{\sigma} = 2\mu\boldsymbol{\varepsilon} + \lambda\boldsymbol{I}\mathrm{tr}(\boldsymbol{\varepsilon}), \qquad \mu = \frac{E}{2(1+\upsilon)}, \qquad \lambda = \frac{\upsilon E}{(1+\upsilon)(1-2\upsilon)}, \tag{13}$$

where μ and λ represent Lamé constants and υ the Poisson's ratio. Note that $\boldsymbol{\varepsilon}$ represents strain. In order to write Hooke's law in terms of the strain rate, linearization in time is required. Subsequently, equation (6) is substituted in the linearized equation in order to write the equation in terms of the velocity vector $\boldsymbol{U}$, resulting in

$$\boldsymbol{\sigma}^{k+1} = \boldsymbol{\sigma}^{k} + \Delta t\big(\mu(\boldsymbol{\nabla U} + (\boldsymbol{\nabla U})^{T}) + \lambda\boldsymbol{I}\mathrm{tr}(\boldsymbol{\nabla U})\big), \tag{14}$$

where k represents the iteration step of the discretised momentum equation for a time step size of Δt.

The viscous-plastic rheology, representing frazil ice in the small-scale model, can also be written in terms of the velocity vector $\boldsymbol{U}$, resulting in

$$\boldsymbol{\sigma}^{k+1} = \eta(\boldsymbol{\nabla U} + (\boldsymbol{\nabla U})^T) + (\zeta - \eta)\boldsymbol{I}\mathrm{tr}(\boldsymbol{\nabla U}) - \boldsymbol{I}\frac{P}{2}. \tag{15}$$

In order to spatially distinguish between the material constituents, we make use of the volume of fluid (VOF) method. The VOF method is a numerical technique, describing the interface between two immiscible and incompressible fluids (Roenby, Bredmose et al. 2016).
Domain size plays an important role, since this paper specifically focusses on small-scale modelling of the dynamics of sea ice in the Antarctic MIZ. What is small-scale modelling of sea ice in this context? Large-scale models in literature refer to domain sizes of 10 to 100 kilometers. Finding the threshold between large-scale and small-scale, is critical to set up the required domain size for the small-scale modelling. This is done by calculating the average stress, average strain rate and average viscosity for different domain sizes. The ratio of total pancake ice to frazil ice occupying the domain stays constant for this convergence analysis. The size of pancake ice does not change as the domain size changes. Once the average is unaffected by changes in the domain size, the transition between small-scale and large-scale modelling has been identified. A relatively small patch of sea ice is best represented numerically by periodic boundary conditions. Ice flux leaving the outlet boundary equals ice flux entering the inlet boundary. Numerically this means that all values of each variable at the outlet boundary are equal to the values of each variable at the inlet boundary (Versteeg 1995).

The variables ice thickness, h, and ice coverage, A, describe a smeared model approach, in which several different types of ice are modelled as one homogeneous material representing averaged quantities. In the small-scale model the variables ice thickness, h, and ice coverage, A, are treated differently. Ice coverage, A, has been replaced by two different ice materials; pancake and frazil ice. Ice thickness, h, is assumed to be time-independent. Both pancake and frazil ice have a constant, but independent ice thickness, since the change in ice thickness in z-direction is negligibly small compared to the size of the domain in x- and y-direction. Hence, equation (10) is not part of the small-scale model, resulting in a simplified equation for the ice strength

$$P = P^* h. \tag{16}$$

The next section shows preliminary numerical results obtained from the small-scale model. First the transition from small-scale to large-scale modelling is determined. Subsequently, results from OpenFOAM are shown and explained.

NUMERICAL RESULTS

In this section two different studies have been conducted. The first study identifies the transition between large-scale and small-scale modelling. As mentioned previously, this is done by considering different domain sizes with constant ratio of total pancake ice to frazil ice occupying the domain. Figure 2 shows three different domain sizes starting from 100x100m to 400x400m. Bigger domain sizes have also been considered, up to 1600x1600m. Red and blue represent pancake ice and frazil ice, respectively.

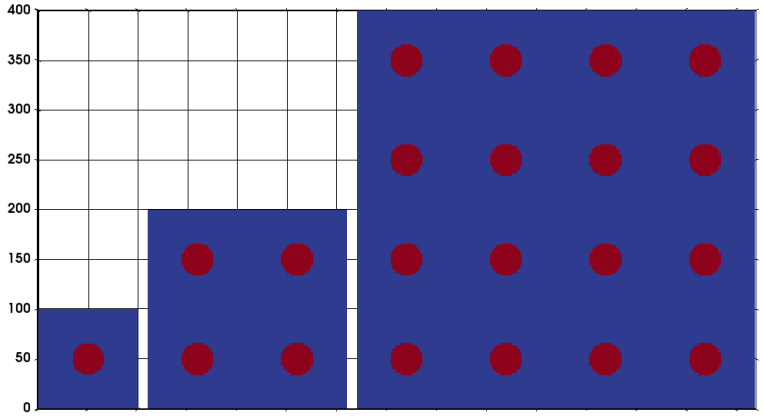

Figure 2. Different domain sizes from 100x100m to 400x400m, with equal ratio of pancake-frazil ice.

For this test case, a constant wind velocity in m/s of $(x, y, z) = (1, -1, 0)$ is considered. Periodic boundary conditions are applied. The VOF method distinguishes pancake ice and frazil ice by the parameter α (Roenby, Bredmose et al. 2016). Cells containing pancake ice and frazil ice have α values of 1 and 0, respectively. All values in between have no physical interpretation; however, these occur because of numerical diffusion; a difficulty encountered in CFD simulations. Cells affected by numerical diffusion are called interface cells. The percentage of interface cells to total domain cells must be of similar magnitude for all domain sizes. To determine the transition between small-scale and large-scale models the average stress, average strain rate and average viscosity are calculated each of which change with an increase in domain size. Once the average is unaffected by changes in the domain size, the threshold has been identified.

In Table 1 percentages are shown of interface cells to total cells for different domain sizes. The percentages highlighted are sufficiently close in order to compare the different domain sizes.

Table 1. Percentage of interface cells to total cells for different domain sizes.

		Domain size [m]				
		100x100	200x200	400x400	800x800	1600x1600
# Cells [-]	3025	**2.38**				
	10000	1.22	**2.34**	4.54	9.69	19.9
	40000	0.60	1.16	**2.41**	4.60	9.53
	160000	0.28	0.57	1.16	**2.41**	4.62
	640000					**2.46**

Figure 3 shows both the effective average stress, σ_{eff} and $\dot{\varepsilon}_{\text{eff}}$ for three different domain sizes. The red and blue lines show the same average values, meaning the transition from small-scale to large-scale has been found at a domain size of approximately 800x800m.

The second study simulates pancake ice modelled as circular shaped ice floes in the small-scale domain of 800x800m for a period of $t = 600\ s$. The ice is exposed to a vortex wind loading moving to the top-right corner of the domain, shown at $t = 0\ s$, $t = 330\ s$ and $t = 600\ s$ in Figure 4.

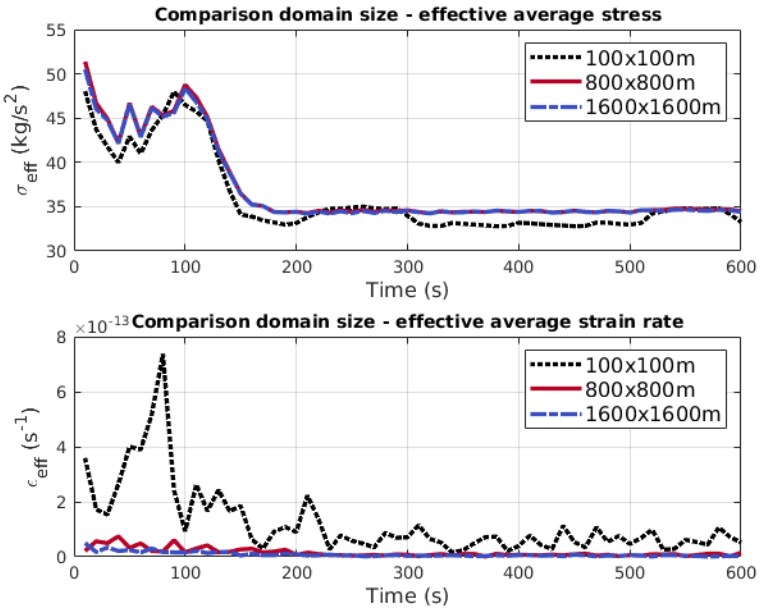

Figure 3. Effective average stress and strain rate for three different domain sizes.

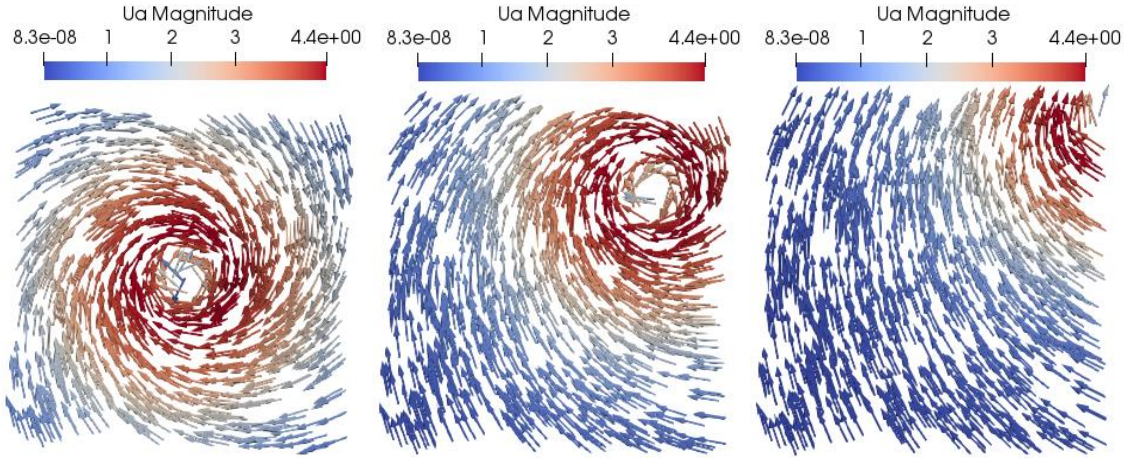

Figure 4. Vortex wind loading moving to the top-right corner of the domain at $t = 0\ s$, $t = 330\ s$ and $t = 600\ s$.

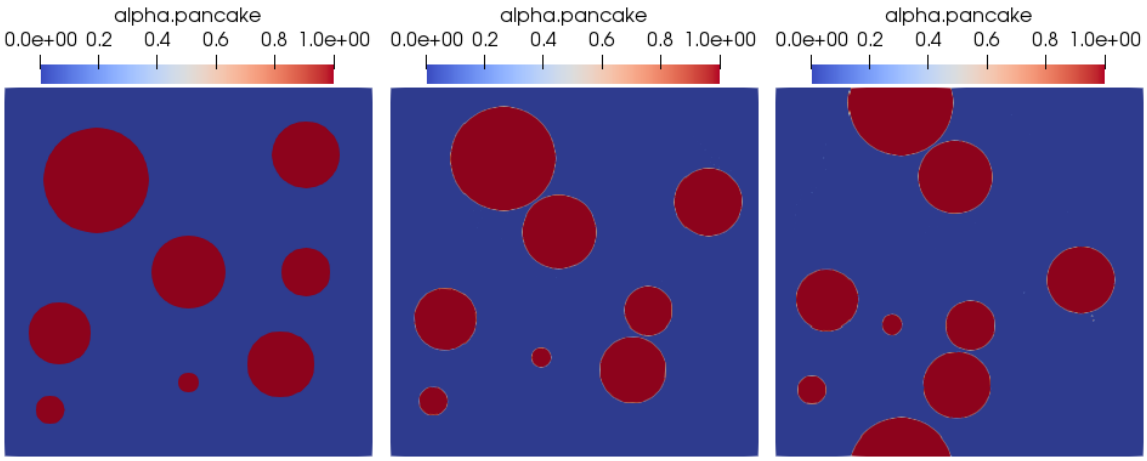

Figure 5. The configuration of pancake ice and frazil ice at $t = 0\ s$, $t = 330\ s$ and $t = 600\ s$ represented by red and blue, respectively.

Figure 5 shows sea ice configuration at $t = 0\ s$, $t = 330\ s$ and $t = 600\ s$. Individual pancake ice floes follow the motion of the vortex and subsequently collide with small deformation. A small layer of frazil ice separates pancake ice during collision. The thickness of the frazil ice layer and the level of compression depend on the material properties of both pancake and frazil ice, given in Table 2. The stress distribution during pancake-pancake ice interaction and pancake-frazil ice interaction at $t = 330\ s$ and $t = 600\ s$ are shown in Figure 6. The latter caps the maximum stresses values to better illustrate the stress distribution in frazil ice. The stress is highest at the interface between pancake ice floes. Pancake ice pushes frazil ice away, resulting in a higher stress at the front of the pancake ice floes and a lower stress behind the pancakes.

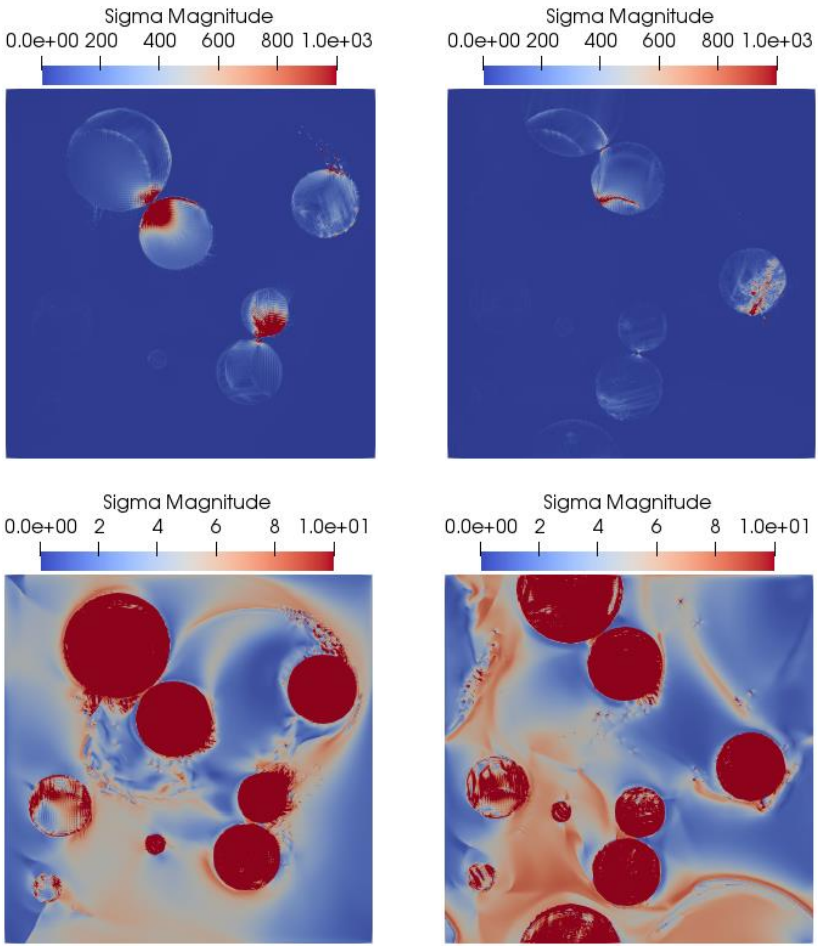

Figure 6. Interaction between pancake and frazil ice at $t = 330\ s$ and $t = 600\ s$.

Some material parameters, like the density and the strength of frazil ice, still need to be accurately determined. A rough estimation of these parameters has been used in the small-scale model. These values will be updated after the Polar Engineering Research Group has extracted sea ice samples from the Antarctic MIZ during the SA Agulhas II winter cruise in 2019. All parameters, including definitions and values can be found in Table 2.

CONCLUSIONS

This paper has shown the promising initial work into the small-scale modelling of sea ice in the Antarctic MIZ. The existing large-scale model by Hibler has been modified on several aspects. Firstly, different ice material constituents are distinguished; pancake ice and frazil ice

with distinct properties. This in contrast to a smeared model approach in which a large fractured sea ice area is modelled as one isotropic, continuous and homogeneous material representing averaged quantities. Secondly, an elastic-viscous-plastic small-scale sea ice rheology has been developed, which allows for both pancake-pancake ice and pancake-frazil ice interaction. Lastly, a vortex wind loading is implemented, derived from Mehlmann and Richter (2017), which provides the flexibility required for realistic modelling of sea ice dynamics.

Table 2. Parameters, definitions and values. p = pancake, f = frazil

Parameter	Definition	Value
$h_{p/f}$	Thickness of ice	0.5 / 0.1 m
$\rho_{p/f}$	Density of ice	918 / 970 kgm^{-3}
$E_{p/f}$	Young's modulus of ice	8.7e9 / 0 kgs^{-2}
$P^*_{p/f}$	Strength of ice	0 / 50 kgm^{-1}s^{-2}
ρ_a	Air density	1.2 kgm^{-3}
ρ_w	Water density	1026 kgm^{-3}
C_a	Air drag coefficient	5e-2
C_w	Water drag coefficient	5e-4
e	Ellipse ratio	2

ACKNOWLEDGEMENTS

This paper, 'Modelling the dynamics of ice in the Antarctic marginal ice zone', is part of a project for a doctoral degree in the field of Civil Engineering, which is carried out within the Polar Engineering Research Group at the University of Cape Town. This research has been supported by the National Research Foundation (NRF) of South Africa (Grant Numbers 104839 and 105858). Opinions expressed, and conclusions arrived at, are those of the author and are not necessarily to be attributed to the NRF.

REFERENCES

Bogaers, A. E. J., G. J. J. v. Rensburg, R. Marquart and S. Skatulla (2018). "Implementation of a visco-plastic sea ice model into OpenFOAM."

Coon, M. D. (1980). A review of AIDJEX modeling. Sea ice processes and models: Proceedings of the Arctic Ice Dynamics Joint Experiment International Commission of Snow and Ice symposium. R. S. Pritchard. Seattle and London, University of Washington Press**:** 12-27.

Dansereau, V., J. Weiss, P. Saramito and P. Lattes (2016). "A Maxwell elasto-brittle rheology for sea ice modelling." Cryosphere **10**(3): 1339-1359.

Feltham, D. L. (2008). "Sea ice rheology." Annual Review of Fluid Mechanics **40**(1): 91-112.

Herman, A. (2016). "Discrete-Element bonded-particle Sea Ice model DESIgn, version 1.3a – model description and implementation." Geoscientific Model Development **9**(3): 1219-1241.

Hibler, W. D. (1979). "A Dynamic Thermodynamic Sea Ice Model." Journal of Physical Oceanography **9**(4): 815-846.

Hunke, E. C. and J. K. Dukowicz (1997). "An elastic-viscous-plastic model for sea ice dynamics." Journal of Physical Oceanography **27**(9): 1849-1867.

Hutchings, J. K., H. Jasak and S. W. Laxon (2004). "A strength implicit correction scheme for the viscous-plastic sea ice model." Ocean Modelling **7**(1-2): 111-133.

Kantha, L. H. (1995). "A Numerical-Model of Arctic Leads." Journal of Geophysical Research-Oceans **100**(C3): 4653-4672.

Massom, R. A. and S. E. Stammerjohn (2010). "Antarctic sea ice change and variability – Physical and ecological implications." Polar Science **4**(2): 149-186.

Mehlmann, C. and T. Richter (2017). "A modified global Newton solver for viscous-plastic sea ice models." Ocean Modelling **116**: 96-107.

Roenby, J., H. Bredmose and H. Jasak (2016). "A computational method for sharp interface advection." R Soc Open Sci **3**(11): 160405.

Thorndike, A. S., D. A. Rothrock, G. A. Maykut and R. Colony (1975). "The thickness distribution of sea ice." Journal of Geophysical Research **80**(33): 4501-4513.

Versteeg, M. (1995). An introduction to computational fluid dynamics.

Wilchinsky, A. V. and D. L. Feltham (2006). "Modelling the rheology of sea ice as a collection of diamond-shaped floes." Journal of Non-Newtonian Fluid Mechanics **138**(1): 22-32.